Available online at www.sciencedirect.com
SCIENCE DIRECT®
ELSEVIER
International Journal of Solids and Structures 42 (2005) 6059–6070
INTERNATIONAL JOURNAL OF SOLIDS and STRUCTURES
www.elsevier.com/locate/ijsolstr

A local search algorithm for natural neighbours in the natural element method

Yongchang Cai *, Hehua Zhu

Department of Geotechnical Engineering, School of Civil Engineering, Tongji University, Shanghai 200092, PR China

Received 28 March 2004; received in revised form 18 April 2005
Available online 4 June 2005

Abstract

A local basis algorithm for searching natural neighbours in Natural Element Method (NEM) is presented for solving the elasticity problems in this paper. Comparison with the global sweep algorithm used in natural element method or Natural Neighbour Method (NNM) for searching natural neighbours, the proposed algorithm is more expedient and convenient in the constructions and computation of natural neighbour interpolations. In the proposed NEM based on local search, the Laplace (non-sibson) interpolations are constructed with respect to the natural neighbour nodes of the given point which have been locally defined. The shape functions from the Laplace approximations have the delta function property and the Laplace interpolants are strictly linear between adjacent nodes, which facilitate imposition of essential boundary conditions and treatment of material discontinuity with ease as it is in the conventional finite element method. The Laplace interpolants derived from the local algorithm and the global algorithm in NEM are identical because of the uniqueness of the Voronoi diagram. Numerical results and convergence studies also show that the present NEM based on local search algorithm possesses the same accuracy and rate of convergence as they are in previous NEM.

Keywords: Meshless; Natural neighbour; Natural element; Laplace interpolation; Element-free

1. Introduction

In recent years, considerable efforts have been devoted to develop various meshless methods to avoid the mesh-related difficulties for certain problems such as crack propagation or large deformations, and about 10 different messless have been developed. A common feature of the meshless methods is that they construct the approximations in terms of discrete nodes and require no predefined nodal connectivity. The common

* Corresponding author. Tel.: +86 21 65983982/65982385; fax: +86 21 65985140.
E-mail addresses: yccai@tongji.edu.cn, yc_cai@163.net (Y. Cai), zhuhehua@tongji.edu.cn (H. Zhu).

0020-7683/$ - see front matter
doi:10.1016/j.ijsolstr.2005.04.006

meshless method, such as the smooth particle hydrodynamic (SPH) by Gingold and Moraghan (1977), reproducing kernel particle method (RKPM) by Liu et al. (1995), element-free Galerkin method (EFG) by Belytschko et al. (1994), meshless local Petrov–Galerkin (MLPG) method by Atluri and Zhu (1998), partition of unity by Melenk and Babuska (1996), Hp-clouds by Duarte and Oden (1996), and finite point method by Onate et al. (1996), are all true meshless methods from the point of view of the node interpolation, and have already been widely applied to various areas (Belytschko et al., 1996, 2000; Liu et al., 2003; Hardee et al., 1999; Li et al., 2002; Ponthot and Belytschko, 1998; Wang et al., 2002). The advantages of these meshless methods are apparent, however serious limitations exist. For instance, the difficulties of imposition of essential boundary and treatment of material discontinuities, uncertain choice of the weight functions, difficulties in the integration of stiffness matrix, and complexity in algorithms for computing the interpolation functions are all major technical problems for stress analysis of solids.

The meshless methods have been proposed to avoid the numerical difficulties of mesh entanglement in the Finite Element Method (FEM), but they pay for the high cost in the computational time, the enforcement of essential boundary, and the treatment of material discontinuities. Special technologies, such as the Penalty method (Zhu and Atluri, 1998), transformation of approximate nodal values to actual nodal values (Cai and Zhu, 2004), nodal integration method (Beissel and Belytschko, 1996; Zhou et al., 2003), combined FEM–EFG method (Belytschko et al., 1995), and efficient computation of shape functions (Beitkopf et al., 2000), have been proposed to overcome the problems. But the progress is miniscule untile recently due to the deficiency of the data interpolation scheme used in these meshless methods.

The Natural Element Method (NEM) proposed by Braun and Sambridge (1995) and Sukumar et al. (1998), Natural Neighbour Method (NNM) proposed by Sukumar et al. (2001) are another class of meshless methods. The interpolation scheme used in this class of methods is known as natural neighbour interpolation. The properties of the natural neighbour interpolation are excellent, such as its delta function property, linear property between adjacent nodes, and well-defined approximation without uncertain user-defined parameter. The NEM presents some distinct and attractive features and has already been applied to various analysis in solid and fluid mechanics.

Instead of searching for the natural neighbours on a global sweep algorithm in NEM, a local search algorithm in natural element method, which quantifies the natural neighbour nodes of the given point based on the locally delaunay triangles, is proposed. The proposed local algorithm is more expedient and convenient in the constructions and computation of natural neighbour interpolations compared with the global sweep algorithm used in previous NEM.

The arrangement of this paper is as follows: the algorithm searching for natural neighbours based on the locally delaunay triangles is presented in Section 2. The computation of the Laplace interpolations is presented in Section 3. In Section 4, the governing equations of elastostatics for NEM based on the local search are described. Section 5 demonstrates the effectiveness of the proposed method by analyzing two linear elastostatics problems. Conclusion are discussed in Section 6.

2. Search for natural neighbours

In order to solve the differential equations of boundary value problems in present NEM, a set of distinct nodes $N = \{n_1, n_2, \ldots, n_m\}$ should first be set up at the arbitrary geometry shape of domain Ω (see Fig. 1).

Suppose that sample point $p(\boldsymbol{x})$ is an arbitrary numerical integral point of domain Ω, the algorithm for the neighbour-search in present NEM is based on the locally delaunay triangles. Let the initial influence nodes $M = \{m_1, m_2, \ldots\}$ of the point p be confined within the dashed lines of the square as shown in Fig. 2.

The next step is to directly determine the natural neighbours of the point p by using the *empty circumcircle criterion* — if $\mathrm{DT}(n_I, n_J, n_K)$ is any Delaunay triangle of the nodal set N, then the circumcircle of DT

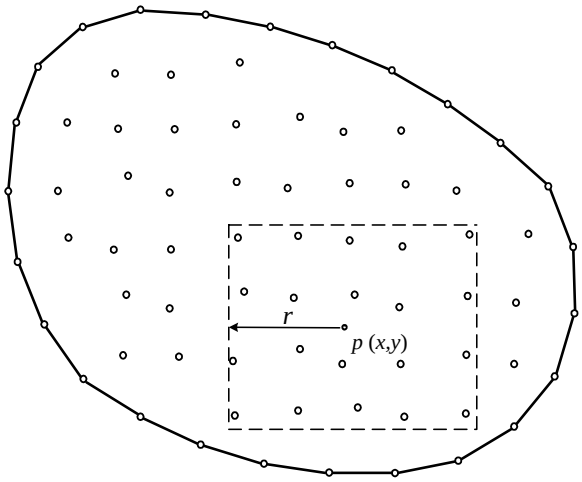

Fig. 1. Discrete model of region Ω and its arbitrary integrate point p ($\boldsymbol{x}$).

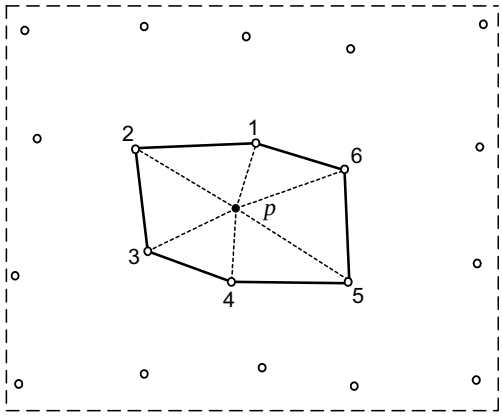

Fig. 2. Natural neighbour of the point p.

contains no other nodes of N. Find the node 1 which is nearest to sample point p from the nodal set M. Starting with edge $p-1$ and using the empty circumcircle criterion, we form a set of locally defined triangles $\{p,1,2\}$, $\{p,2,3\}$, $\{p,3,4\}$, $\{p,4,5\}$, and $\{p,5,6\}$, where the nodes 1–6 are selected from the nodal set M in Fig. 2. Now, the nodes 1–6 are just the natural neighbours of the point p.

The natural neighbours of the given point p are unique after the nodal set N has been set up at the domain Ω. The size of the square edges $2r$ in Fig. 1 will not and can not influence the definition of the natural neighbours of point p. The purpose of the restriction of the influence nodes to the square region is to reduce the time for searching for the natural neighbours. Hence, the size of the length r must be large enough to contain all the natural neighbours of point p, and should be small enough to save the time consumed of the neighbour-search. Of course, the nodal set N of domain Ω can be regarded as the initial influence nodal set M of the point p, but the neighbour-search will be much more expensive and can not be afforded.

In Sukumar (2003) and Sukumar et al. (2001), the neighbour-search of the point p is different from the above algorithm. The sequence of the key steps for neighbour-search is as follows. At first, the Delaunay triangulation of the domain Ω is constructed by connecting the nodes using the empty circumcircle

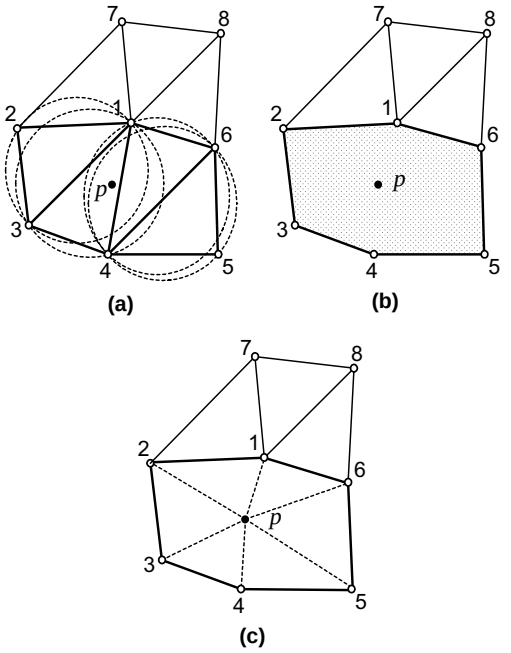

Fig. 3. The step for neighbour-search in NNM.

criterion. Given a point p, the Delaunay triangles that violate the circumcircle criterion (p lies inside the circumcircle of the triangle) are found (Fig. 3(a)). The new triangles (Fig. 3(c)) for the computation of the laplace interpolant can be formed by deleting the interior edges of the associated triangles (Fig. 3(b)) and connecting p to the facets on the outer boundary.

Clearly, the natural neighbours of the point p in Figs. 2 and 3(c) are the same. The important difference of the neighbour-search methods is that the complex and robost alogrithm of the Voronoi diagram for the whole domain Ω is not needed in the present NEM.

3. Laplace interpolation

Natural neighbours provide a means to define a robust appoximation for scattered nodes in Ω according to the relative spatial density and position of nodes. Silbson and Laplace (non-silbson) natural neighbour interpolations can be differently used in NEM. In 2D, the Laplace shape function defined by the ration of length measures (Sukumar et al., 2001) whereas the Silbson shape function is based on the ration of areas (Sukumar et al., 1998). The computational cost and algorithm are more favorable in Laplace interpolant than in Silbson interpolant. In this paper, we choose Laplace interpolant to develop the NEM.

In Fig. 4, C_{12p}, C_{23p}, C_{34p}, C_{45p}, C_{56p}, and C_{61p} are the circumcentres of the triangles $\{p,1,2\}$, $\{p,2,3\}$, $\{p,3,4\}$, $\{p,4,5\}$, $\{p,5,6\}$, and $\{p,6,1\}$, respectively. Connecting the points $\{C_{12p}, C_{23p}, C_{34p}, C_{45p}, C_{56p}, C_{61p}\}$ by sequence, we can form the voronoi cell of the point p. If the point $p(\boldsymbol{x})$ has n natural neighbours (six neighbours in Fig. 4), then the Laplace shape function for node i is defined as:

$$\Phi_i(\boldsymbol{x}) = \frac{\alpha_i(\boldsymbol{x})}{\sum_{j=1}^{n} \alpha_j(\boldsymbol{x})}, \quad \alpha_j(\boldsymbol{x}) = \frac{s_j(\boldsymbol{x})}{h_j(\boldsymbol{x})}, \quad \boldsymbol{x} \in R^2 \tag{1}$$

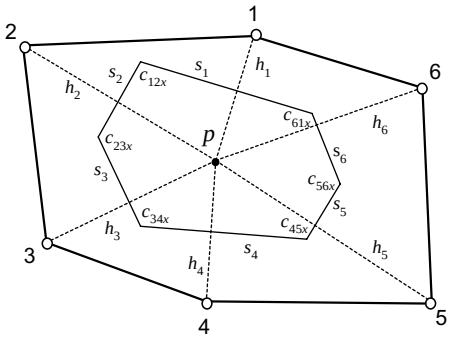

Fig. 4. Computation of Laplace interpolation of the natural neighbours.

where $\alpha_j(\boldsymbol{x})$ is the Laplace weight function, $s_j(\boldsymbol{x})$ is the length of the voronoi edge associated with point p and node i, and $h_j(\boldsymbol{x})$ is the Euclidean distance between point p and node i (Fig. 4).

The derivatives of the coordinates are obtained by differentiating Eq. (1):

$$\begin{aligned}\Phi_{i,j}(\boldsymbol{x}) &= \frac{\alpha_{i,j}(\boldsymbol{x}) - \Phi_i(\boldsymbol{x})\alpha_{,j}(\boldsymbol{x})}{\alpha(\boldsymbol{x})} \\ \alpha(\boldsymbol{x}) &= \sum_{k=1}^{n} \alpha_k(\boldsymbol{x}), \alpha_{,j}(\boldsymbol{x}) = \sum_{k=1}^{n} \alpha_{k,j}(\boldsymbol{x})\end{aligned} \tag{2}$$

The global forms of displacement approximations $\boldsymbol{u}^h(\boldsymbol{x})$ of point $p(\boldsymbol{x})$ can be written as

$$\boldsymbol{u}^h(\boldsymbol{x}) = \sum_{i=1}^{n} \Phi_i(\boldsymbol{x})\boldsymbol{u}_i \tag{3}$$

where $\boldsymbol{u}_i (i = 1, \ldots, n)$ are the vectors of nodal displacements at the n natural neighbours of point p, and $\Phi_i(\boldsymbol{x})$ are the shape functions associated with each node.

By defining of the shape function given in Eq. (1), the following properties are self-evident

$$\sum_{i=1}^{n} \Phi_i(\boldsymbol{x}) = 1, \quad \boldsymbol{x} \in \Omega \tag{4}$$

$$\begin{cases} 0 \leqslant \Phi_i(\boldsymbol{x}) \leqslant 1, \\ \Phi_i(\boldsymbol{x}_j) = \delta_{ij}, \end{cases} \boldsymbol{x} \in \Omega \tag{5}$$

From Eq. (5), it can be seen that the Laplace interpolation passes through the nodal values, which is in contrast to most meshless approximations, where the nodal parameters $\boldsymbol{u}_i$ are not nodal displacements. Also, the Laplace shape functions is C^0 at nodal locations as well as on the boundary of the support. These properties make that the Laplace interpolant exactly satisfy (linear) essential boundary conditions. A more detailed discussion of the Laplace interpolation and its application to PDEs can be found in Sukumar et al. (2001) and the references therein.

It is noted that if the position of the point p is the same as an arbitrary node i, the algorithm in Eq. (1) will fail because of the Euclidean distance $h_j(\boldsymbol{x}) = 0$ and Laplace weight function $\alpha_i(\boldsymbol{x}) = \pm\infty$. This situation never arises when the triangular finite elements are used as integral cell and all integration points are interior to the triangles. But when the regular cells, for example, the cells in Fig. 5 similar to the EFG method, are used to the integral scheme, the computational difficulty is encountered. A generally applicable method to overcome this numerical difficulty is to randomly move nodes by a small distance (e.g. 1e-10) before computing.

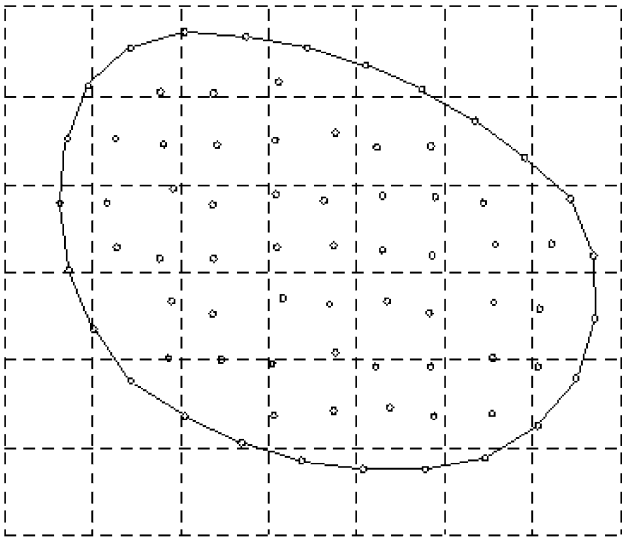

Fig. 5. The regular background cells for numerical integration.

4. Discrete equations

We consider the two-dimensional problem with small displacements on the domain Ω bounded by Γ. The equilibrium equation and boundary conditions are given as follows:

$$\nabla \cdot \boldsymbol{\sigma} + \boldsymbol{b} = 0, \text{ in } \Omega \tag{6a}$$

$$\boldsymbol{\sigma} \cdot \boldsymbol{n} = \bar{\boldsymbol{t}}, \quad \text{on } \Gamma_t \tag{6b}$$

$$\boldsymbol{u} = \bar{\boldsymbol{u}}, \quad \text{on } \Gamma_u \tag{6c}$$

where $\boldsymbol{\sigma}$ is the stress tensor which corresponds to the displacement filed $\boldsymbol{u}$;$\boldsymbol{b}$ is the body force vector; the superposed bar in (6b) and (6c) denotes prescribed boundary values, and $\boldsymbol{n}$ is the unit normal to the domain.

The variational form of (6) is posed as follows

$$\int_{\Gamma_t} \delta \boldsymbol{u} \cdot \boldsymbol{t} \, \mathrm{d}\Gamma - \int_{\Omega} \delta \varepsilon \cdot \boldsymbol{\sigma} \, \mathrm{d}\Omega + \int_{\Omega} \delta \boldsymbol{u} \cdot \boldsymbol{b} \, \mathrm{d}\Omega = 0 \quad \forall \delta \boldsymbol{u} \in \boldsymbol{H}_0^1 \tag{7}$$

The discretized system can be obtained by substituting (1) into (7)

$$\boldsymbol{K} \cdot \boldsymbol{D} = \boldsymbol{f} \tag{8}$$

where

$$\boldsymbol{K}_{IJ} = \int_{\Omega} \boldsymbol{B}_I^T \cdot \boldsymbol{DE} \cdot \boldsymbol{B}_J \, \mathrm{d}\Omega \tag{9}$$

$$\boldsymbol{f}_{\boldsymbol{I}} = \int_{\Gamma_t} \Phi_{\boldsymbol{I}} \cdot \boldsymbol{t} \, \mathrm{d}\Gamma + \int_{\Omega} \Phi_{\boldsymbol{I}} \cdot \boldsymbol{b} \, \mathrm{d}\Omega \tag{10}$$

where $\boldsymbol{DE}$ is the elasticity matrix, $\boldsymbol{B}_{\boldsymbol{I}}$ is the strain matrix.

From the above deduction,we can know that the numerical results obtained by NEM with Laplace interpolants (Sukumar et al., 2001) and the present NEM with local search are the same because the Laplace interpolants derived from both algorithm are identical due to the uniqueness of the Voronoi diagram.

The algorithm for the neighbour-search is the only difference in previous NEM in Sukumar et al. (2001) and present NEM in this paper.

5. Numerical examples

The present NEM is coded in standard C++. Cases are run in order to examine the NEM in two dimensional elastostatics.

The patch test of the present NEM based on local search is the same as the previous NEM and NNM based on global search. The accuracy of the finite element type in the patch test in NEM cannot be expected due to the fact that the numerical integration of the weak form is inexact as it is in EFG and other meshless methods.

In order to evaluate the error in the solutions, we define the displacement norm and energy norm as follows:

$$\|\boldsymbol{u}\| = \left(\int_{\Omega} \boldsymbol{u}^T \cdot \boldsymbol{u}\, \mathrm{d}\Omega\right)^{\frac{1}{2}} \tag{11}$$

$$\|\boldsymbol{\varepsilon}\| = \left(\int_{\Omega} \boldsymbol{\varepsilon}^T \cdot \boldsymbol{\sigma}\, \mathrm{d}\Omega\right)^{\frac{1}{2}} \tag{12}$$

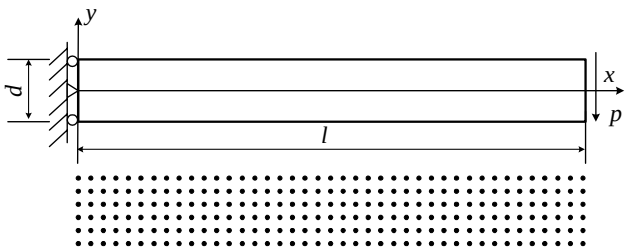

Fig. 6. Cantilever beam and its nodes distribution.

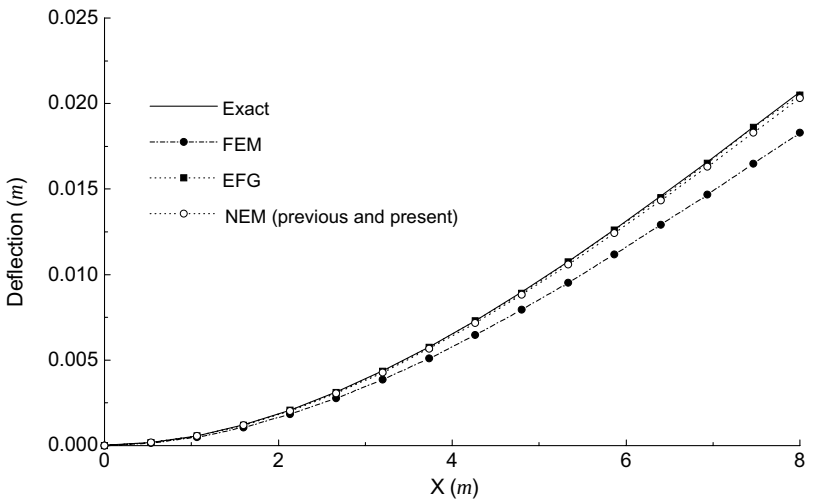

Fig. 7. Comparison of deflection y at $y = 0$.

The relative errors for $\|\boldsymbol{u}\|$ and $\|\boldsymbol{\varepsilon}\|$ are defined as:

$$r_u = \frac{\|\boldsymbol{u}^{\text{num}} - \boldsymbol{u}^{\text{exact}}\|}{\|\boldsymbol{u}^{\text{exact}}\|} \tag{13}$$

$$r_e = \frac{\|\boldsymbol{\varepsilon}^{\text{num}} - \boldsymbol{\varepsilon}^{\text{exact}}\|}{\|\boldsymbol{\varepsilon}^{\text{exact}}\|} \tag{14}$$

5.1. Cantilever beam

Consider a beam of length $l = 8$ m and height $b = 1$ m as shown in Fig. 6. The displacements are prescribed at $x = 0$ and a parabolic traction $P = 1N$ is applied to the free end. The analytical solution to this

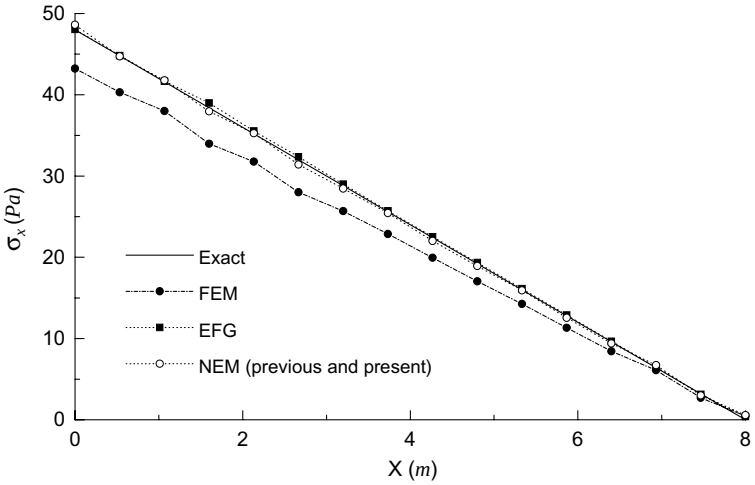

Fig. 8. Comparison of normal stress σ_x.

Table 1
Comparison of computational cost (unit:s)

	Nodes	Mesh	Search for cover node	Computational of strain matrix	Assemble and solve equation	Total
1506	FEM	0.19	–	0.21	0.48	0.88
	Previous NEM	0.19	0.31	0.29	1.06	1.85
	Present NEM	–	0.57	0.29	1.06	1.92
	EFG	–	0.37	0.45	1.49	2.31
3847	FEM	0.57	–	0.63	0.78	1.98
	Previous NEM	0.57	1.07	1.21	3.12	5.97
	Present NEM	–	1.83	1.21	3.12	6.16
	EFG	–	1.24	1.73	4.85	7.82
6009	FEM	1.03	–	1.09	1.44	3.56
	Previous NEM	1.03	1.74	3.10	5.35	11.22
	Present NEM	–	3.16	3.10	5.35	11.61
	EFG	–	1.93	4.65	7.97	14.55

problem is shown in Belytschko et al. (1994). The material properties are $E = 1 \times 10^5$ Pa and $v = 0.25$. The problem is solved for the plane stress case.

The comparisons of the deflection v and the stress σ_x at $y = 0$ with 246 distinct nodes are shown in Figs. 7 and 8. It can be found from Figs. 7 and 8 that the numerical solutions of displacement and stress obtained by EFG and present NEM show a good agreement with the exact solution which is much better than those obtained by triangular FEM.

The time required in numerical computations in a same computer is compared with that in triangular FEM, EFG, previous NEM, and present NEM. The subsequent results are shown in Table 1. In present NEM, the mesh step is not needed, but the time for neighbour search is grater than it is in previous NEM. As seen from Table 1, the time required in present NEM is almost the same of the previous

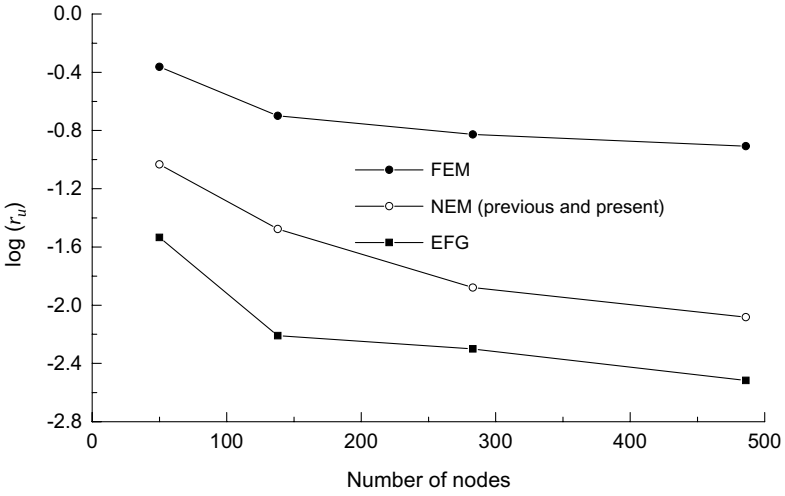

Fig. 9. Convergence of relative displacement error norm for beam problem.

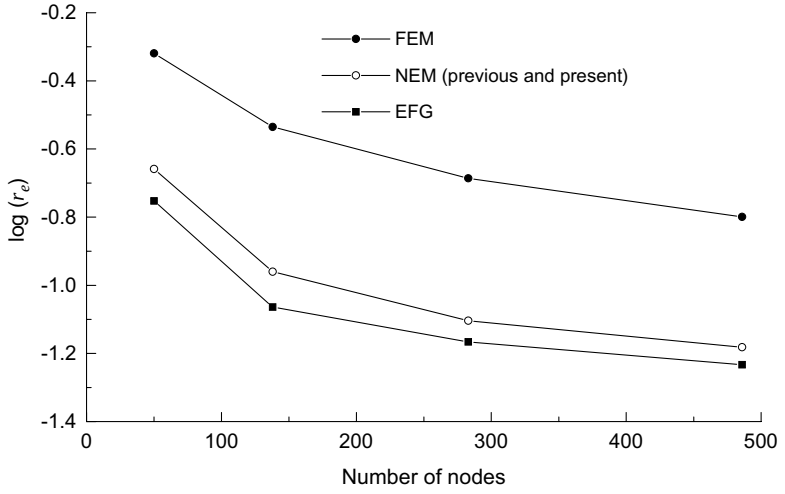

Fig. 10. Convergence of relative energy error norm for beam problem.

NEM, greater than triangular FEM, and a little shorter than EFG. We can find that the local search-algorithm in the present NEM can not improve the computational efficient of natural neighbour interpolations. The merits of the present NEM lie in its expedience in the constructions and computation of natural neighbour interpolations and convenience for nonlinear and large deformation problems for which iterative methods are needed.

The convergence study is performed using 50, 138, 283, and 486 node discretizations. Convergence in displacement is shown in Fig. 9, and convergence of energy is reported in Fig. 10. High convergence rates have been achieved in the present method.

5.2. Infinite plate with a hole

This problem is a portion of an infinite plate with a central circular hole (Fig. 11). An unidirectional tensile load of $\sigma = 1$ Pa in the x direction is applied at the boundary. Due to symmetries only the upper right

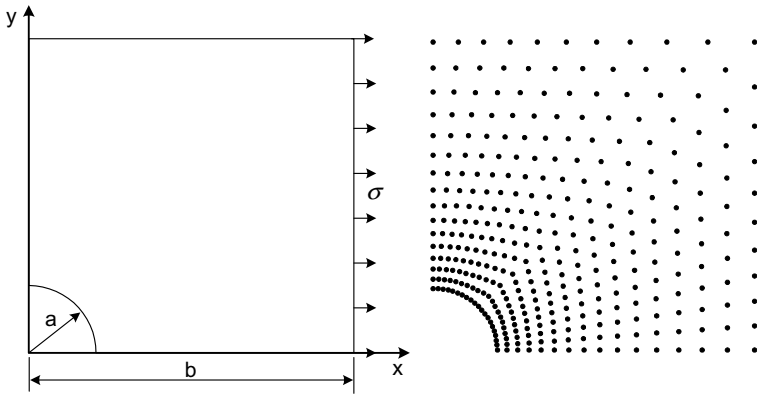

Fig. 11. Infinite plate with central hole and its nodes distribution.

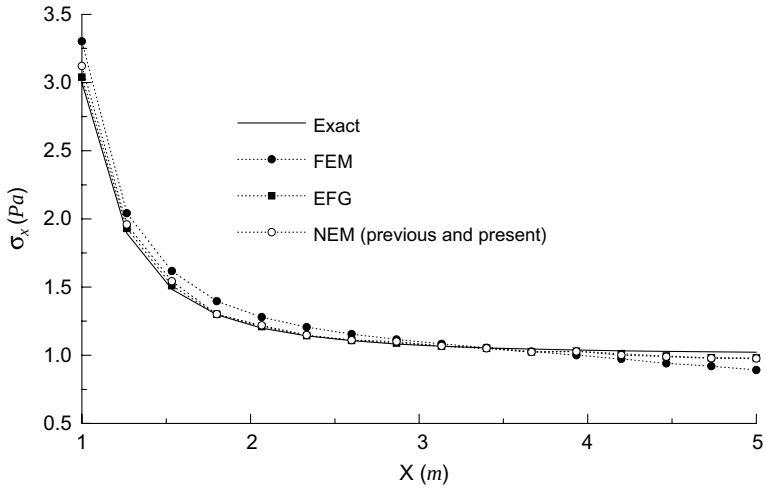

Fig. 12. Comparison of normal stress σ_x at $x = 0$ for the infinite plate with central hole problem.

Table 2
Comparison of computational cost (unit:s)

	Nodes	Mesh	Search for cover node	Computational of strain matrix	Assemble and solve equation	Total
1276	FEM	0.15	–	0.18	0.48	0.81
	Previous NEM	0.15	0.29	0.25	0.96	1.65
	Present NEM	–	0.49	0.25	0.96	1.70
	EFG	–	0.32	0.41	1.26	1.99
3512	FEM	0.54	–	0.59	0.75	1.88
	Previous NEM	0.54	1.02	1.19	3.08	5.83
	Present NEM	–	1.76	1.19	3.08	6.03
	EFG	–	1.19	1.71	4.65	7.55
6532	FEM	1.14	–	1.21	1.61	3.96
	Previous NEM	1.14	1.91	3.29	5.54	11.88
	Present NEM	–	3.44	3.29	5.54	12.27
	EFG	–	2.10	4.93	8.18	15.21

quadrant is modeled with $a = 1$ m and $b = 5$ m. The comparison of stress σ_x at $x = 0$ with 336 distinct nodes is given in Fig. 12. The time comparisons of different methods are shown in Table 2.

6. Conclusion

A local basis algorithm in natural element method for solving elastostatic problems, which searches the natural neighbour nodes of the given point and have been defined based on the locally delaunay triangles, is proposed. A variational form is used to form the system discrete equation for two-dimensional solids. Comparison of the computational time indicates that the present NEM based on local search is feasible and attractive.

The main benefits of present NEM are:

- The complex and robost algorithm for whole domain Ω is not needed and the proposed algorithm is more expedient and convenient in the constructions and computation of natural neighbour interpolations.
- Some difficulties in other meshless methods ,such as, the implementation of essential boundary condition and treatment of material discontinuities, have been avoided.

These advantages allow the present NEM to be one of the simplest meshless method to implement, especially for solving the problems of crack propagation or large deformations. Numerical examples demonstrate the same effectiveness and accuracy have been achieved in the previous NEM based on global search and the present NEM for elastostatics.

References

Atluri, S.N., Zhu, T., 1998. A new meshless local Petrov–Galerkin (MLPG) approach in computational mechanics. Computational Mechanics 22, 117–127.

Beissel, S., Belytschko, T., 1996. Nodal integration of the element-free Galerkin method. Computer Methods in Applied Mechanics and Engineering 139, 49–74.

Belytschko, T., Krongauz, Y., Organ, D., 1996. Meshless methods:An overview and recent developments. Computer Methods in Applied Mechanics and Engineering 139, 3–47.

Belytschko, T., Lu, Y.Y., Gu, L., 1994. Element-free Galerkin method. International Journal for Numerical Methods in Engineering 37, 229–256.

Belytschko, T., Organ, D., Gerlach, C., 2000. Element-free Galerkin methods for dynamic fracture in concrete. Computer Methods in Applied Mechanics and Engineering 187, 385–399.

Belytschko, T., Organ, D., Krongauz, Y., 1995. A Coupled finite element-element free Galerkin method. Computational Mechanics 17, 186–195.

Beitkopf, P., Rassineux, A., Gibert, T., et al., 2000. Explicit form and efficient computation of MLS shape functions and their derivatives. International Journal for Numerical Methods in Engineering 48, 451–466.

Braun, J., Sambridge, M., 1995. A numerical method for solving partial differential equations on highly irregular evolving grids. Nature 376, 655–660.

Cai, Y.C., Zhu, H.H., 2004. Direct imposition of essential boundary condition and treatment of material discontinuity in EFG method. Computational Mechanics 34, 330–338.

Duarte, C.A., Oden, J.T., 1996. Hp clouds: A h-p meshless method. Numerical Methods for Partial Differential Equations 12, 673–705.

Gingold, R.A., Moraghan, J.J., 1977. Smoothed particle hydrodynamics: Theory and applications to non-spherical stars. Monthly Notice of the Royal Astronomical Society 18, 375–389.

Hardee, E., Chang, K.H., Grindeanu, I., et al., 1999. A Structure Nonlinear Analysis Workspace based on meshless method. Advances in Engineering Software 30, 153–175.

Li, S.F., Liu, W.K., Rosakis, A.J., et al., 2002. Mesh free Galerkin simulations of dynamic shear band propagation and failure mode transition. International Journal of Solids and Structures 39, 1213–1240.

Liu, W.K., Jun, S., Zhang, Y.F., 1995. Reproducing Kernel Particle methods. International Journal for Numerical Methods in Fluids 20, 1081–1106.

Liu, M.B., Liu, G.R., Zong, Z., et al., 2003. Computer simulation of high explosive explosion using Smoothed particle hydrodynamics methodology. Computers & Fluids 32, 305–322.

Melenk, J.M., Babuska, I., 1996. The partition of unity finite element methods: Basic theory and application. Computer Methods in Applied Mechanics and Engineering 139, 263–288.

Onate, E., Idelsohn, S., Zienkiewicz, O.C., et al., 1996. A finite point method in computational mechanics: Applications to convective transport and fluid flow. International Journal for Numerical Methods in Engineering 39, 3839–3866.

Ponthot, J.P., Belytschko, T., 1998. Arbitrary Lagrangian–Eluerian formulation for element-free Galerkin method. Computer Methods in Applied Mechanics and Engineering 152, 19–46.

Sukumar, N., 2003. Voronoi cell finite difference method for the diffusion operator on arbitrary unstructured grids. International Journal for Numerical Methods in Engineering 57, 1–34.

Sukumar, N., Moran, B., Belytschko, T., 1998. The natural element method in solid mechanics. International Journal for Numerical Methods in Engineering 43, 839–887.

Sukumar, N., Moran, B., Semenov, Y., 2001. Natural neighbour Galerkin method. International Journal for Numerical Methods in Engineering 50, 1–27.

Wang, J.G., Liu, G.R., Lin, P., 2002. Numerical analysis of Biot's consolidation process by radial point interpolation method. International Journal of Solids and Structures 39, 1557–1573.

Zhou, J.X., Wen, J.B., Zhang, H.Y., et al., 2003. A nodal integration and post-processing technique based on Voronoi diagram for Galerkin meshless methods. Computer Methods in Applied Mechanics and Engineering 192, 3831–3843.

Zhu, T., Atluri, S.N., 1998. A modified collocation method and a penalty formulation for enforcing the essential boundary conditions in the element free Galerkin method. Computational Mechanics 21, 211–222.